A novel slotted helix slow-wave structure for high power Ka-band traveling-wave tubes*

Liu Lu-Wei(刘鲁伟)[a], Wei Yan-Yu(魏彦玉)[a]†, Wang Shao-Meng(王少萌)[a], Hou Yan(侯 艳)[a], Yin Hai-Rong(殷海荣)[a], Zhao Guo-Qing(赵国庆)[a], Duan Zhao-Yun(段兆云)[a], Xu Jin(徐 进)[a], Gong Yu-Bin(宫玉彬)[a], Wang Wen-Xiang(王文祥)[a], and Yang Ming-Hua(杨明华)[b]

[a] *National Key Laboratory of Science and Technology on Vacuum Electronics, University of Electronic Science and Technology of China, Chengdu* 610054, *China*
[b] *Beijing Vacuum Electronics Research Institute (BVERI), Beijing* 100016, *China*

(Received 6 December 2012; revised manuscript received 17 April 2013)

A novel slotted helix slow-wave structure (SWS) is proposed to develop a high power, wide-bandwidth, and high reliability millimeter-wave traveling-wave tube (TWT). This novel structure, which has higher heat capacity than a conventional helix SWS, evolves from conventional helix SWS with three parallel rows of rectangular slots made in the outside of the helix tape. In this paper, the electromagnetic characteristics and the beam-wave interaction of this novel structure operating in the Ka-band are investigated. From our calculations, when the designed beam voltage and beam current are set to be 18.45 kV and 0.2 A, respectively, this novel circuit can produce over 700-W average output power in a frequency range from 27.5 GHz to 32.5 GHz, and the corresponding conversion efficiency values vary from 19% to 21.3%, and the maximum output power is 787 W at 30 GHz.

Keywords: slotted helix, slow-wave structure, millimeter-wave, traveling-wave tube, beam-wave interaction

PACS: 84.40.Fe, 84.47.+w, 07.57.Hm **DOI:** 10.1088/1674-1056/22/10/108401

1. Introduction

Millimeter-wave radiation sources, specifically at the Ka-band frequency, with high powers, wide-bandwidths, high efficiencies, and miniaturizations are attractive for many applications, such as high-data-rate communications, radar, space applications, and electronic warfare.[1–10] One of the most promising millimeter-wave amplifiers that can satisfy the above requirements is the helix TWT due to its unique ability to provide wide-bandwidth interaction with an extremely compact and lightweight structure. However, because of its high thermal resistance in the helix SWS, the heat dissipation capability of the helix SWS is restricted, and the typical output power from helix TWTs is lower than those from other types of vacuum electron device (VED) amplifiers.[11–13] In recent years, with the application of new techniques and materials, helix TWTs operating in the Ka-band can provide over 500 W average output power.[14–16] However, the thermal design of the helix SWS is still one of the main limiting factors to obtaining high-power millimeter-wave helix TWTs.[17]

In order to improve the heat dissipation capability of the helix SWS, a novel slotted helix SWS[18] has been proposed for high power TWTs. This structure is derived from the idea of increasing the thickness of the conventional helix tape, and then three parallel rows of rectangular slots spaced 120° apart are made in the outside of the helix tape. The slot can increase the contact area between the helix tape and the support rod; thus the heat produced by RF loss and electronic bombardment can be conducted out quickly. Our preliminary thermal and electromagnetic analysis of this structure show that it has better heat dissipation capability than and similar high frequency characteristic to the conventional helix SWS.[19] Therefore, based on the novel slotted helix SWS, high power and high reliability millimeter wave helix TWTs are expected.

In this paper, the thermal analysis and RF properties of the novel slotted helix SWS are calculated by using ANSYS,[20] HFSS,[21] and CST Microwave Studio[22] software. Subsequently, the beam-wave interaction simulations of the novel slotted helix slow-wave circuit are conducted by utilizing CST Particle Studio.[23]

2. System description

Figure 1 shows a three-dimensional model of the novel slotted helix SWS, which consists of a copper plated slotted helix tape made of molybdenum, three dielectric support rods made of beryllia and a copper plated stainless steel shell. The rectangular support rods are inserted into the slots tightly within the shell, and then the novel structure is assembled by using the diffusion brazing method.[24] Thus, the novel structure not only has higher heat capacity, but also higher stability than that of a conventional helix SWS.

*Project supported by the National Natural Science Foundation of China (Grant No. 61271029), the Natural Science Key Laboratory Foundation, and the Natural Science Fund for Distinguished Young Scholars of China (Grant No. 61125103).

†Corresponding author. E-mail: yywei@uestc.edu.cn

© 2013 Chinese Physical Society and IOP Publishing Ltd

Figure 2 shows the dimensional parameters of the slotted helix SWS, wherein a is the inner radius of the slotted helix tape, s is the thickness of the helix tape, h is the depth of the slot, c is the inner radius of the shell, d is the width of the support rod, w is the width of the helix, and p is the pitch of the helix tape.

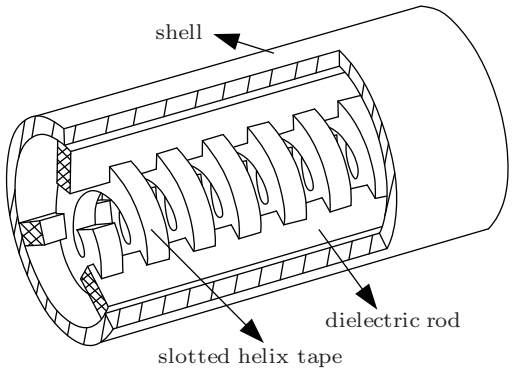


Fig. 1. Three-dimensional model of the slotted helix SWS.

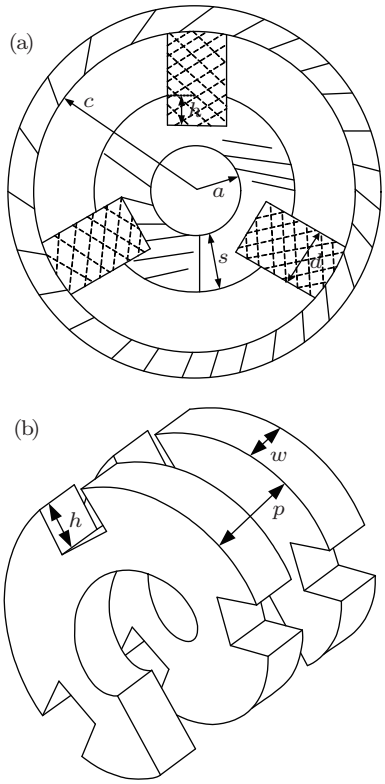


Fig. 2. Dimensional parameters of the slotted helix SWS: (a) cross section of the slotted helix SWS, (b) three-dimensional model of the slotted helix tape.

3. Thermal analysis of the slotted helix SWS

In this section, thermal analysis of the novel slotted helix SWS is simulated by using ANSYS software. Steady state thermal analysis is used to simulate the circuit response in this paper. The optimized structural parameter values of the slotted helix SWS are presented in Table 1.

Table 1. Optimized structural parameters.

Parameter	Value
a/s	1.5
h/s	0.5
c/s	4
d/s	1
w/s	1.8
p/w	2

In the simulations, the last ten helix turns of the novel slow-wave circuit are selected to perform the thermal analysis, where the largest temperature gradient has been found in experiments. By applying the boundary conditions and thermal load as described in Ref. [25], the simulations can be performed very well. Here, in order to describe the superiority of the novel slotted helix SWS, the thermal analysis of the conventional helix SWS is also calculated for comparison under the same condition except that the thickness of the helix tape a/s is equal to 3.

Figure 3 shows a comparison of heat dissipation capability between the conventional and the novel helix SWS. As can be seen, under the same dissipation power, especially when the dissipation power is larger, the maximum temperature of the novel helix tape is smaller than that of the conventional one. That is to say, the novel structure has higher heat capacity than a conventional helix SWS.

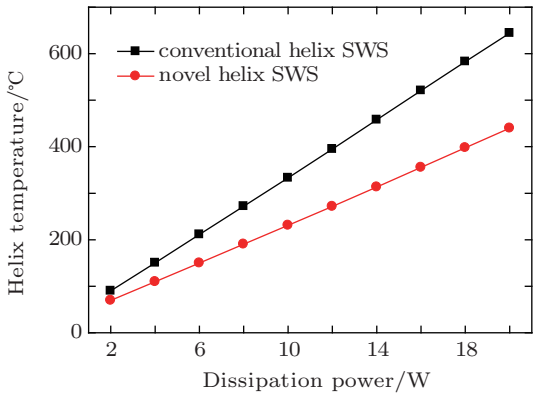


Fig. 3. (color online) Comparison of heat dissipation capability between the conventional and the novel helix SWS.

4. RF properties

In this section, the RF properties including high frequency characteristics and transmission characteristics are investigated. The high frequency characteristics of this structure are calculated by means of HFSS, which refers to the dispersion characteristics and beam-wave interaction impedance. Because the novel slotted helix SWS has a periodic structure, the simulation can be carried out only in one pitch. By employing master and slave boundary condition[26] in the eigenmode solver, the simulation can be conducted and optimized in an efficient and accurate way. Figure 4(a) shows the dispersion characteristics of the novel helix SWS, which indicate that this

structure is a fundamental forward wave circuit and the electron beam interacts with the zero space harmonic. Interaction impedance versus frequency of the fundamental mode at the zero space harmonic is given in Fig. 4(b).

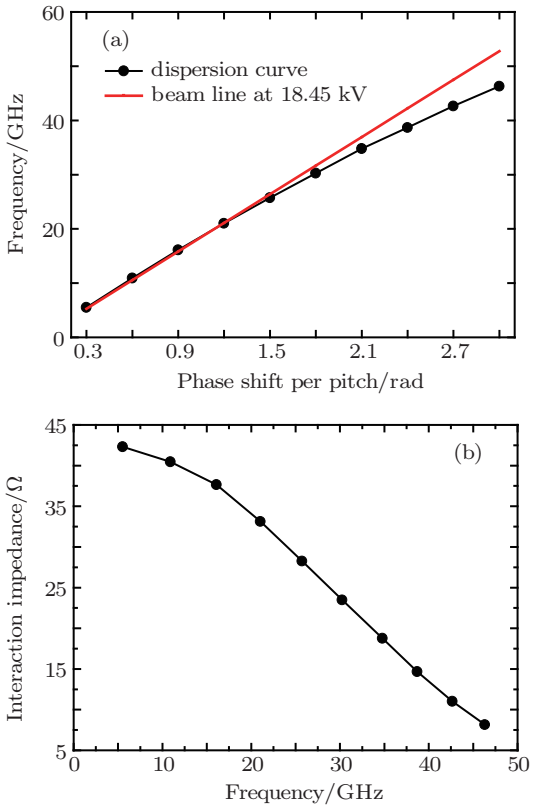


Fig. 4. (color online) (a) Dispersion characteristics with synchronous beam voltage line. (b) Interaction impedance of the slotted helix SWS.

Using the transient solver in the Microwave Studio of the CST, the transmission characteristics of the novel helix circuit can be calculated. The novel circuit is comprised of fifty turns of the helix SWS with input and output coupling structure. In our simulations, the electrical conductivity of the copper plated helix tape is 5.8×10^7 S/m, the relative permittivity of the dielectric rod is 6.5, and the boundary is specified as being of copper with a conductivity of 5.8×10^7 S/m. The simulation result is shown in Fig. 5. It can be seen from Fig. 5 that the reflection parameters S_{11} are smaller than -20 dB ranging from 21 GHz to 39 GHz. The maximum transmission loss S_{21} is about 0.03 dB/mm.

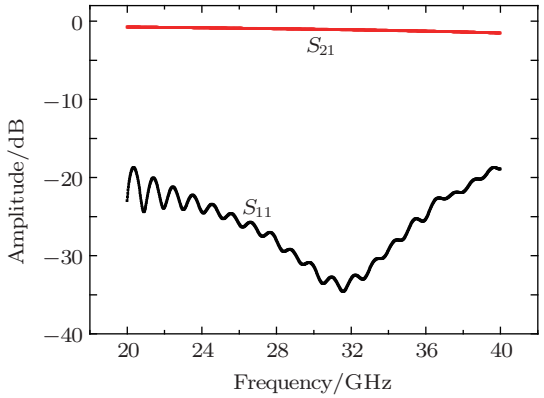


Fig. 5. (color online) Transmission characteristics of the novel circuit.

5. Beam-wave interaction simulations

In this section, the beam-wave interaction simulations of the novel slotted helix slow-wave circuit are investigated by utilizing CST Particle Studio based on the optimized parameters given above. In order to obtain a large gain and suppress backward wave oscillation, the whole circuit is divided into two sections and two concentrated attenuators made of carburized porous beryllia with a relative permittivity and high loss tangent of 6.5 and 0.5 are used in the interaction circuit as shown in Fig. 6(a). Here, the first section consists of 65 periods and the second section consists of 84 periods, and output ports 2 and 3 are the ideal match ports, which can monitor the signal power that has not been absorbed by concentrated attenuator. These two ports are very helpful for the optimal design of the whole interaction circuit. Figure 5(b) shows the attenuation profiles along the interaction length. In order to absorb the electromagnetic wave very well, the attenuations of the attenuators in the first section and in the second section are set to be 25 dB and 28 dB, respectively.

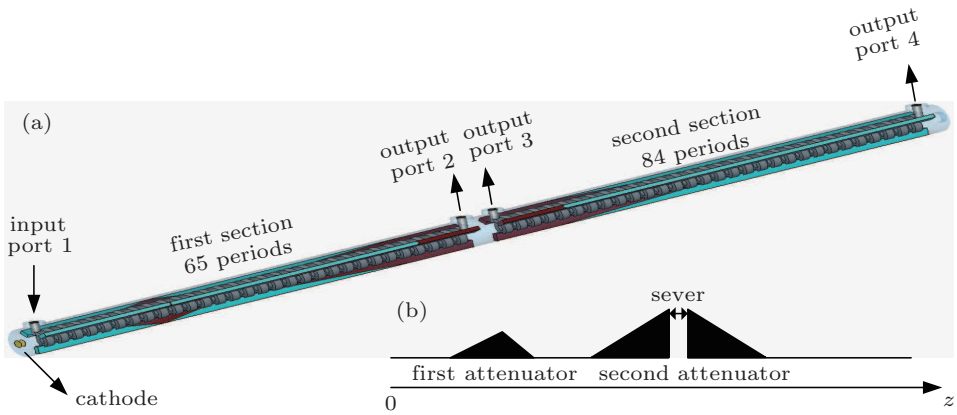


Fig. 6. (color online) (a) Three-dimensional model of the complete tube with an attenuator and a server. (b) The lower right inset gives the attenuator profile along the interaction length.

In order to improve electronic efficiency, a negative phase velocity tapering (PVT) approach is used to design the helix slow-wave circuit.[27–29] The whole novel RF circuit consists of an input section L_0 with pitch P_0 followed by an increased phase velocity section L_1 with pitch P_1 and then a negative tapered section L_2 with pitch P_2 as shown in Fig. 7. The purpose of the negative PVT approach is that section L_1 gathers the electrons into bunches as effectively as possible and section L_2 extracts the energy from the bunched beam as effectively as possible, so electronic efficiency can be greatly improved.

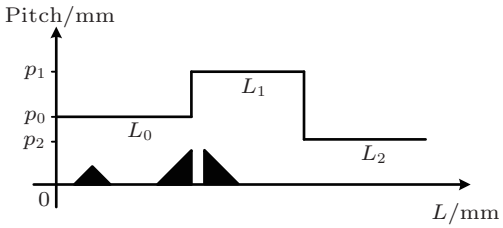


Fig. 7. Optimal pitch profile versus distance for the TWT.

In the simulations, a uniform longitudinal focusing magnetic field of 0.35 T is used here to confine the electron beam, and the electron beam filling factor is set to be 0.65. Through the optimization calculations, when $p_1/p_0 = 1.056$, $p_2/p_1 = 0.92$, and $L_1/L_2 = 2.565$, the novel RF circuit has a maximum average output power. And the optimized operating parameters for the novel helix TWT are shown in Table 2.

Table 2. Optimized parameters for a 30-GHz TWT.

Parameter	Value
Beam voltage	18.45 kV
Beam current	0.2 A
Center frequency	30 GHz
Input power	54.45 mW
Saturated output pwoer	787 W
Saturated gain	41.6 dB
Saturated efficiency	21.3%

The performances of the TWT operating at a representative frequency of 30 GHz are shown in Figs. 8 and 9. Figure 8(a) shows the power transfer curve. It is shown that when the input power is smaller, the average output power increases linearly, that is to say, the TWT works in a small signal state. However, as the input power continues to increase, the TWT will work in a nonlinear state. When the input power is 54.45 mW, the TWT can be driven up to a saturated state with a maximum average output power of 787 W. Figure 8(b) depicts the time-domain features of the input signal and the output signal monitored at output port 4. It can be seen that the output signal takes about 2.5 ns to become stable, and no oscillation is observed.

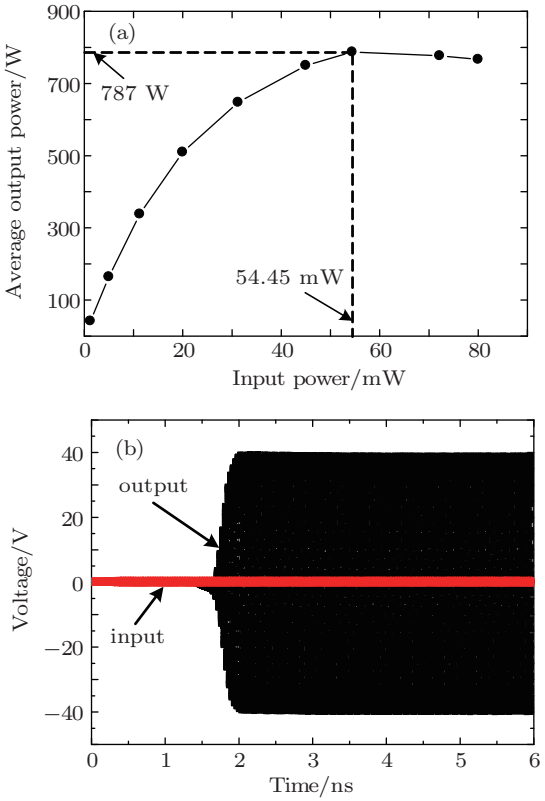


Fig. 8. (color online) (a) Power transfer curve. (b) Input signal and the PIC simulation result of the output signal monitored at output port 4.

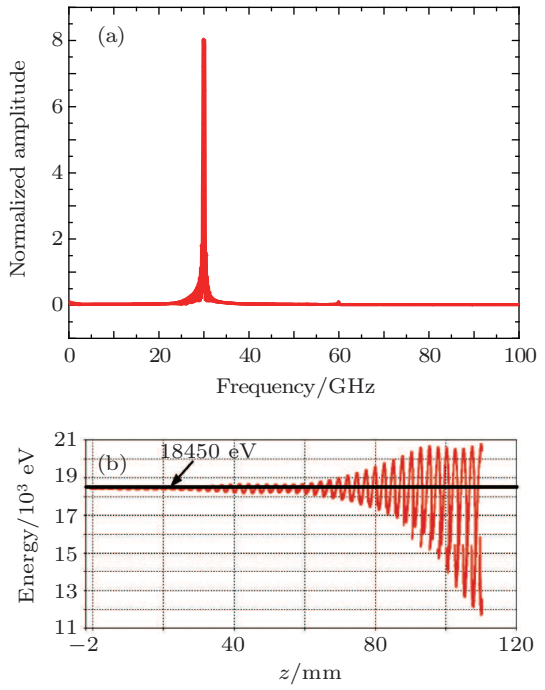


Fig. 9. (color online) (a) Frequency spectrum of output signal. (b) Stable phase space plot of the bunched electron beam at 5.5 ns.

Figure 9(a) shows the frequency spectrum of the output signal monitored at output port 4. As can be seen, the output signal spectrum is concentrated around 30 GHz and is relatively pure. Although the higher harmonics are also aroused at around 60 GHz, the amplitudes are much lower than that of

operating frequency of 30 GHz. Figure 9(b) shows the phase space plot of the bunched electron beam along the axial distance at 5.5 ns when the electron dynamic system is already in a steady state. As can be seen, most of the electrons are decelerated and a smaller number of the electrons are accelerated at the end of the circuit, which indicates that the kinetic energy of the electron beam is transferred to the high-frequency electromagnetic field very well.

In the same way, the instantaneous bandwidth of this TWT can be calculated with the same input power. The average output power, gain, and electronic efficiency versus drive frequency are shown in Fig. 10. It is shown that the novel slotted helix TWT can produce over 700 W average output power in a frequency range from 27.5 GHz to 32.5 GHz, the corresponding conversion efficiency values vary from 19% to 21.3%, and the maximum average output power is 787 W at 30 GHz. Especially, the gain changes of 0.5 dB within the 5-GHz bandwidth can satisfy the requirements of many applications, such as space communication, electronic warfare, etc.

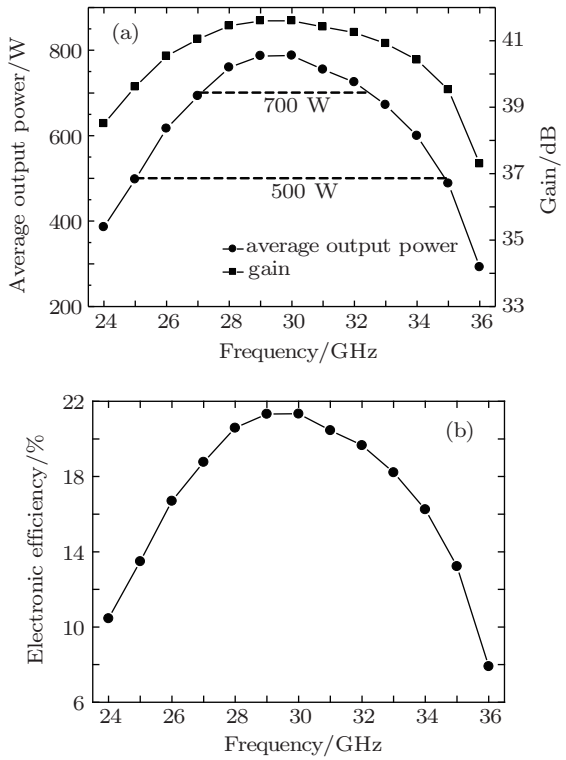


Fig. 10. (a) Plots of average output power and gain versus frequency. (b) Electronic efficiency versus frequency.

6. Conclusion

In this paper, a slotted helix SWS is investigated. According to the simulation results, the novel slotted helix TWT can produce over 700-W average output power in a frequency range from 27.5 GHz to 32.5 GHz with a gain change of only 0.5 dB. Besides, the slotted helix SWS has higher heat dissipation capability and higher reliability than a conventional helix SWS, thus it is a promising slow-wave structure for developing wideband, high gain, high-power, and high reliability millimeter-wave TWTs. Future work will be concentrated on the experiment study of this novel slotted helix SWS.

References

[1] Feng J J, Hu Y F, Cai J, Wu X P and Tang Y 2010 *Vacuum Electronics* **52** 27 (in Chinese)
[2] Komm D S, Benton R T, Limburg H C, Menninger W L and Zhai X L 2001 *IEEE Trans. Electron Dev.* **48** 174
[3] He J, Wei Y Y, Gong Y B, Duan Z Y and Wang W X 2010 *Acta Phys. Sin.* **59** 2843 (in Chinese)
[4] He J, Wei Y Y, Gong Y B, Duan Z Y, Lu Z G and Wang W X 2010 *Acta Phys.* Sin. **59** 6659 (in Chinese)
[5] He J, Wei Y Y, Gong Y B and Wang W X 2011 *Chin. Phys. B* **20** 054102
[6] Gao X, Yang Z Q, Cao W P and Jiang Y N 2011 *Chin. Phys. B* **20** 030703
[7] Feng J J, Cai J, Hu Y F, Wu X P, Ma S Y and Qu B 2009 *Institute of Chinese Electronics Conference on Microwave Tubes*, p. 5 (in Chinese)
[8] Xie H Q and Liu P K 2006 *Chin. Phys.* **15** 2042
[9] Smirnova E I, Carlsten B E and Earley L M 2008 *IEEE Trans. Plasma Sci.* **36** 763
[10] Peng W F, Hu Y L, Yang Z H, Li J Q, Lu Q R and Li B 2011 *Chin. Phys. B* **20** 028401
[11] Li Z L, Feng J J, Wang E F and Liu B T 2010 *Vacuum Electronics* **52** 41 (in Chinese)
[12] Wang Y 2004 *J. Appl. Opt.* **25** 57 (in Chinese)
[13] Guo J H, Yu S, Li H F, Zhang T Z, Lei C J, Li X and Zhang Y Y 2011 *Acta Phys. Sin.* **60** 090301 (in Chinese)
[14] Chong C K, Dawson R C, Forster J W, Le Borgne R H, Ramay M L, Stolz R J and Tamashiro R N 2008 *Proc. IEEE Int. Vac. Electron. Conf.*, April 22–24, 2008, Monterey, USA, p. 191
[15] Boshch E, Christ R, Lefevre M, Racamier J, Rupp H, Tribout J and Jarno J 2009 *Proc. IEEE Int. Vac. Electron. Conf.*, April 28–30, 2009, Rome, Italy, p. 70
[16] Machida T, Suzuki W, Yoshida M, Matsuoka J and Tsutaki K 2011 *Proc. IEEE Int. Vac. Electron. Conf.*, February 21–24, 2011, Bangalor, India, p. 17
[17] Chong C K, Davis J A, Borgne R H L, Ramay M L, Stolz R J, Tamashiro R N, Vaszari J P and Zhai X L 2005 *IEEE Trans. Electron Dev.* **52** 653
[18] Wei Y Y, Liu L W, Gong Y Y, Xu X, Yin H R, Yue L N, Liu Y and Wang W X, U.S. Patent 13 345 121
[19] Liu L W, Wei Y Y, Xu X, Shen F, Zhao G Q, Huang M Z, Tang T, Wang W X and Gong Y B 2012 *Proc. 5th Global Symposium on Millimeter Waves Conf.*, May 27–30, 2012, Harbin, China, p. 312
[20] Ansoft ANSYS, Inc., *Analysis Guide*, Release 14.0, 2012
[21] Ansoft Corp., *Ansoft HFSS User's Reference*, http://www.ansoft.com.cn/
[22] CST Corp., *CST MWS Tutorials* [online] available: http://www.cst-china.cn/
[23] CST Corp., *CST PS Tutorials* [online] available: http://www.cst-china.cn/
[24] Han Y, Liu Y W, Ding Y G and Liu P K 2008 *IEEE Electron Dev. Lett.* **29** 955
[25] Han Y, Liu Y W, Ding Y G and Liu P K 2009 *Acta Phys. Sin.* **58** 1806 (in Chinese)
[26] Booske J H, Converse M C, Kory C L, Chevalier C T, Gallagher D A, Kreischer K E, Heinen V O and Bhattacharjee S 2005 *IEEE Trans. Electron Dev.* **52** 685
[27] Duan Z Y, Gong Y B, Lu M Y, Wei Y Y and Wang W X 2008 *Chin. Phys. Lett.* **25** 934
[28] Srivastava V, Carter R G, Ravinder B, Sinha A K and Joshi S N 2000 *IEEE Trans. Electron Dev.* **47** 2438
[29] Jung S S, Soukhov A V, Jia B F and Park G S 2002 *Appl. Phys. Lett.* **80** 3000